

THE DRAMATIC SIZE EVOLUTION OF ELLIPTICAL GALAXIES AND THE QUASAR FEEDBACK

L. FAN^{1,2}, A. LAPI^{3,1}, G. DE ZOTTI^{4,1}, AND L. DANESE¹

Draft version May 26, 2019

ABSTRACT

Observations have evidenced that passively evolving massive galaxies at high redshift are much more compact than local galaxies with the same stellar mass. We argue that the observed strong evolution in size is directly related to the quasar feedback, which removes huge amounts of cold gas from the central regions in a Salpeter time, inducing an expansion of the stellar distribution. The new equilibrium configuration, with a size increased by a factor $\gtrsim 3$, is attained after ~ 40 dynamical times, corresponding to ~ 2 Gyr. This means that massive galaxies observed at $z \geq 1$ will settle on the Fundamental Plane by $z \sim 0.8-1$. In less massive galaxies ($M_\star \lesssim 2 \times 10^{10} M_\odot$), the nuclear feedback is subdominant, and the mass loss is mainly due to stellar winds. In this case, the mass loss timescale is longer than the dynamical time and results in adiabatic expansion that may increase the effective radius by a factor of up to ~ 2 in 10 Gyr, although a growth by a factor of $\simeq 1.6$ occurs within the first 0.5 Gyr. Since observations are focused on relatively old galaxies, with ages $\gtrsim 1$ Gyr, the evolution for smaller galaxies is more difficult to perceive. Significant evolution of velocity dispersion is predicted for both small and large galaxies.

Subject headings: Galaxies: formation - galaxies: evolution - galaxies: elliptical - galaxies: high redshift - quasars: general

1. INTRODUCTION

Several recent observational studies have found that massive, passively evolving, galaxies at $z > 1$ are much more compact than local galaxies of analogous stellar mass (Ferguson et al. 2004; Trujillo et al. 2004, 2007; Cimatti et al. 2008; Damjanov et al. 2008). Since similarly superdense massive galaxies are extremely rare or absent at $z \simeq 0$ (Shen et al. 2003) a strong size evolution, by a factor ~ 3 or more, is indicated. No convincing mechanism able to account for such size evolution has been proposed so far. In the following we show that an expansion consistent with the observed one is naturally expected as a consequence of feedback from active nuclei (Silk & Rees 1998; Granato et al. 2001, 2004), which is now widely recognized as a crucial ingredient of semi-analytic models (see, e.g., Di Matteo et al. 2008).

In the local Universe spheroidal galaxies occupy a quite narrow region, the Fundamental Plane, in the 3-dimensional space identified by the effective or half-light radius r_e , by the central velocity dispersion σ_0 , and by the mean surface brightness within r_e (Djorgovski & Davis 1987). The tight color-magnitude relation, the color-velocity dispersion relation, and spectral line indices imply that the bulk of stars of elliptical galaxies formed at $z \geq 1.5$. The enhancement of α -elements abundances with respect to iron in massive elliptical galaxies entails that most of their stars formed within the first Gyr of their life (see Renzini 2006 for a comprehensive discussion).

An additional key result is the generic presence of a Super Massive Black Hole (SMBHs) in the center of local elliptical galaxies. Its mass is directly proportional to the mass of the old stellar population, $M_{\text{BH}} \sim 2 \times 10^{-3} M_\star$ (Magorrian et al 1998; see Ferrarese & Ford 2005 for a review), implying

that quasars and spheroidal galaxies form and evolve in strict relation and with mutual feedback. Specifically, it has been suggested that the central SMBH grows until its feedback unbinds the residual gas in the host galaxy and sweeps it out through a high velocity wind, thus halting both the star formation and its own fueling and establishing a relationship between the SMBH mass and the stellar velocity dispersion (Silk & Rees 1998). Strong AGN feedback also appears to be the only viable mechanism to explain the exponential cut-off at the bright end of the galaxy luminosity function (Croton et al. 2006) and the observed bimodality in the color-magnitude diagram of galaxies at $z \gtrsim 1.5$ (Menci et al. 2006). Direct observational indications of massive outflows close to high redshift quasars, consistent with this scenario, have been reported (e.g. Simcoe et al. 2006; Prochaska & Hennawy 2008).

As shown below, the amount of gas rapidly stripped from the central regions of the galactic halo can be large enough to drive a large increase of the galaxy size. The puffing up of a system by rapid mass loss is a well known phenomenon, extensively studied both analytically and through numerical simulations, with reference to galaxies (Biermann & Shapiro 1979), and, especially, to globular clusters (Hills 1980; Goodwin & Bastian 2006). Slower, adiabatic expansion is caused by mass loss due to stellar winds or supernova explosions (Hills 1980; Richstone & Potter 1982).

In this *Letter* we first summarize the effect of mass loss on the galaxy size evolution (§ 2), then we present quantitative estimates on the evolution of the effective radius and of the central stellar velocity dispersion as a function of galactic mass, using the Granato et al. (2004) model as a reference (§ 3), and finally, in § 4, we summarize and discuss our results.

2. SIZE EVOLUTION DUE TO MASS LOSS FROM VIRIALIZED SYSTEMS

The effect of the mass loss on the structure and dynamics of a virialized stellar system depends on the amount of ejected mass and on the timescale of ejection. Two regimes can be identified, corresponding to an ejection timescale, τ_{ej} , shorter or longer than the dynamical timescale τ_{dyn} .

¹ Astrophysics Sector, SISSA/ISAS, Via Beirut 2-4, 34014 Trieste, Italy

² Center for Astrophysics, University of Science and Technology of China, Hefei, 230026, China

³ Dip. Fisica, Univ. “Tor Vergata”, Via Ricerca Scientifica 1, 00133 Roma, Italy

⁴ INAF-Osservatorio Astronomico di Padova, Vicolo dell’Osservatorio 5, 35122 Padova, Italy

2.1. Rapid mass loss

A rapid mass loss ($\tau_{\text{ej}} < \tau_{\text{dyn}}$) results in a shallower potential well at essentially constant velocity dispersion. If M and M' are the initial and final masses, the final energy, E' , of a spherical system is related to the initial energy E by $E' = E(M'/M)^2(2 - M/M')$ (Biermann & Shapiro 1979), so that if $M/M' > 2$ the system has positive energy and is unbound. If $M/M' < 2$, the system will eventually relax to a new equilibrium configuration. If the latter is homologous to the initial one, the ratio of initial (R) to final (R') radii is

$$R/R' = 2 - M/M'. \quad (1)$$

Numerical simulations essentially confirm this simple estimate and show that, if the system is not disrupted, the new equilibrium configuration is reached after about 30–40 initial dynamical times (see, e.g., Goodwin & Bastian 2006).

It is important to note that the above argument assumes that the system is self-gravitating and isolated. Clearly the dark matter (DM) halo, which extends far beyond the stellar distribution, exerts a stabilizing action and prevents its disruption.

2.2. Long lasting, adiabatic mass loss

If the mass loss occurs on a timescale $\tau_{\text{ej}} > \tau_{\text{dyn}}$, the system expands through the adiabatic invariants of the orbits of stars, and the expansion proceeds at a rate proportional to the mass loss rate (Hills, 1980; Richstone & Potter 1982). We have:

$$R'/R = M/M'. \quad (2)$$

In this case no global disruption of the system is possible and the velocity is inversely proportional to the size.

3. MASS LOSS AND SIZE EVOLUTION OF HIGH REDSHIFT GALAXIES

Observations of (sub)-millimeter bright QSOs, thought to be close to the onset of the massive outflows determining the transition from the active star-forming phase to the unobscured QSO phase, indicate very large gas masses in the central regions of their host galaxies (Lutz et al. 2008, and references therein), comparable to the stellar masses (Coppin et al. 2008). Similar star to gas ratios are found in the central regions of sub-mm bright galaxies (Tacconi et al. 2008).

About 5% of the QSO bolometric luminosity during the maximum quasar activity is enough to remove the gas in about one Salpeter time ($\simeq 4 \times 10^7$ yr), through outflows of $\dot{M} \gtrsim 1,000 M_\odot \text{ yr}^{-1}$ (e.g. Granato et al. 2004). The high precision spectroscopy of the QSO SDSSJ1204+0221 by Prochaska & Hennawi (2008) is indeed consistent with a high velocity ($v \simeq 1,000 \text{ km s}^{-1}$), massive outflow of $\dot{M} \sim 3,000 M_\odot \text{ yr}^{-1}$.

There are thus both observational indications and theoretical arguments for the occurrence of the conditions leading to the expansion described in § 2.1. For sake of definiteness, we will present quantitative estimates exploiting the model by Granato et al. (2004), which reproduces the crucial observational features of the coevolution of quasars and elliptical galaxies (see Lapi et al. 2006 for a comprehensive discussion). In this model, both the star formation and the growth of the SMBH proceed faster in more massive halos, in keeping with the observed “downsizing”. In the most massive galaxies, the quasar feedback quenches the star formation after ~ 0.5 Gyr, thus accounting for the observed α -enhancement. The star formation occurs in the inner regions of the galactic halo, encompassing a fraction ≤ 20 –30% of the baryons associated to the halo. The star formation may be triggered

and enhanced by the rapid merging of a few sub-halos. The dynamical friction is able to dissipate angular momentum of the collapsing baryons, transferring it to DM particles. The numerical simulations by El-Zant et al. (2001) showed that dynamical friction between baryon and DM clouds within the scale radius of the Navarro et al. (1997) density distribution ($r \leq r_s$) is strong enough to overcome the expected adiabatic contraction of DM caused by the deepening of the potential well under the influence of the shrinking baryons. Eventually the central regions are gravitationally dominated by baryons (stars and cold gas), that may share the velocity field of the DM clouds (cfr. Fig. 3 of El-Zant et al. 2001). Under more general assumptions, the baryon collapse is expected to result in stellar velocity dispersions somewhat higher than those of the DM. We set $\sigma_* \approx f_\sigma \sigma_{\text{DM}}$.

We can assume that the stars and the cold gas, of mass M_* and M_{cold} respectively, are in virial equilibrium just before the mass loss. Neglecting the DM contribution to the mass in the central region, its gravitational radius can be expressed as $r_g \approx G(M_* + M_{\text{cold}})/\sigma_*^2$ and the dynamical time scale of the collapsed baryon component is $\tau_{\text{dyn}} = (\pi/2)(r_g/\sigma_*)$.

If we adopt a Sérsic’s (1968) law for the projected stellar density profile, the effective radius, that we identify with the projected half stellar mass radius, is related to the gravitational one by $r_e = S_s(n)r_g$, and the observed luminosity weighted central velocity dispersion is related to the global density-weighted velocity dispersion by $\sigma_0^2 = S_K(n) < \sigma^2$, where n is the Sérsic index ($n = 4$ for a de Vaucouleurs (1959) $r^{-1/4}$ law). Both $S_s(n)$ and $S_K(n)$ are rather weak function of n tabulated by Prugniel & Simien (1997); in particular, $S_s(4) \simeq 0.34$ and $S_K(4) \simeq 0.52$.

For a Navarro et al. (1997) profile, the halo circular velocity, V_H , and the virial radius r_{vir} are well approximated by $V_H \simeq 230(M_H/10^{12}M_\odot)^{1/3}[(1+z)/4]^{1/2} \text{ km s}^{-1}$ and $r_{\text{vir}} = 80(M_H/10^{12}M_\odot)^{1/3}[(1+z)/4]^{-1} \text{ kpc}$, respectively. If the density profile has a scale length r_s , the DM velocity dispersion is $\sigma_{\text{DM}} = f(c)^{1/2}V_H$, $f(c) \approx 1$ being a weak function of the concentration $c = r_{\text{vir}}/r_s$. Rearranging, we obtain the dynamical time and the effective radius as a function of virial radius and mass of the host halo, and of the mass in stars and in cold gas at the onset of the mass loss:

$$r_e \approx \frac{S_s(4)}{f_\sigma^2} \frac{(M_* + M_{\text{cold}})}{M_H} r_{\text{vir}}. \quad (3)$$

The model gives the mass in stars and in gas, and the mass loss for any choice of the galaxy halo mass, M_H , and of the virialization redshift. We can then compute the effective radius with eqs. (3) and its evolution with eqs. (1) and (2). The application of the virial theorem, using the coefficients $S_s(4)$ and $S_K(4)$, allows us to derive the central line-of-sight velocity dispersion in different evolutionary phases. The results are shown in Fig. 2.

Simple analytical approximations for the mass in stars and cold gas as a function of halo mass and redshift were derived Mao et al. (2007, Appendix A) in the framework of the Granato et al. (2004) model. The key timescales of the model are the condensation time of the cold gas out of the hot phase at virial temperature, $t_{\text{cond}} \approx 9 \times 10^8 [(1+z)/4]^{-1.5} (M_H/10^{12}M_\odot)^{0.2} \text{ yr}$, and the duration of the star formation phase before the onset of the quasar super-wind, $\Delta t_{\text{burst}} \approx 6 \times 10^8 [(1+z)/4]^{-1.5} F(M_H/10^{12}M_\odot) \text{ yr}$, where $F(x) = 1$ for $x \geq 1$ and $F(x) = x^{-1}$ for $x < 1$. The mass

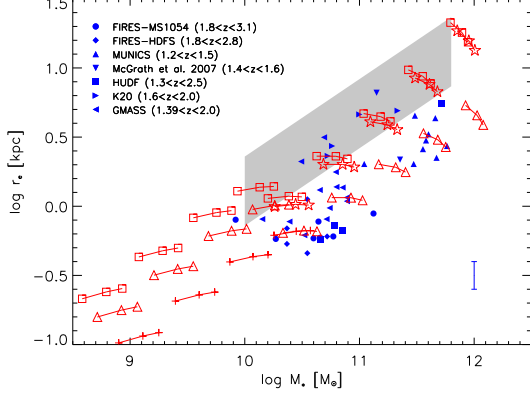


FIG. 1.— Effective radius versus stellar mass. For $M_* \geq 2 \times 10^{10} M_\odot$ triangles, asterisks, and squares show, respectively, the values of r_e : at the end of the bright quasar phase; when the system has reached a new virial equilibrium; at the present time. For $M_* \leq 2 \times 10^{10} M_\odot$ crosses, triangles, and squares show, respectively, the values of r_e : just at the end of baryon collapse; after further 0.5 Gyr; at the present time. The three connected symbols refer to different halo virialization redshifts ($z_{\text{vir}} = 2, 4$, and 6); smaller values of r_e correspond to higher values of z_{vir} . The grey area marks the $\pm 1\sigma$ local size– M_* relation (Shen et al. 2003). Data points as in Fig. 15 of Cimatti et al. (2008). A typical error bar is shown in the lower right-hand corner.

in stars formed during the burst is

$$M_*/M_H \sim s \frac{f_b}{s\gamma - 1} [1 - \exp(-\Delta t_{\text{burst}}/t_{\text{cond}})], \quad (4)$$

where $f_b \simeq 0.18$ is the cosmic baryon to DM density ratio and the function $\gamma \simeq 1 - R + 0.6(M_H/10^{12} M_\odot)^{-2/3}[(1+z)/4]^{-1}$ incorporates the supernova feedback effect. The ratio between the condensation time and the characteristic time of star formation $s = t_{\text{cond}}/t_* \simeq 5$ accounts for the clumping of the gas distribution; $R \simeq 0.3$ denotes the fraction of mass restituted by dying stars to the ISM. During the last e-folding time the quasar activity ejects the residual cold gas, which amounts to

$$\frac{M_{\text{cold}}}{M_*} \simeq \frac{M_{\text{ej}}}{M_*} \approx [s(\exp(\Delta t_{\text{burst}}/t_{\text{cond}}) - 1)]^{-1}. \quad (5)$$

For massive galaxies hosted in halos of $M_H \gtrsim 10^{12} M_\odot$, $M_{\text{cold}}/M_* \sim 2/3$. The ejection of a mass $\simeq M_{\text{cold}}$ can then produce a factor $\simeq 3$ increase in galaxy size (cfr. eq. (1)). On the other hand, for smaller galaxies ($M_H < 10^{12} M_\odot$ and present day stellar mass $M_* < 2 \times 10^{10} M_\odot$) the nuclear activity is much weaker and occurs later, when the ratio M_{cold}/M_* , and hence M_{ej}/M_* , is small. This is in keeping with the general picture that the early evolution of small galaxies is ruled by SN feedback, while the evolution of the large ones is controlled by quasar feedback (see, e.g., Shankar et al. 2006).

4. DISCUSSION AND CONCLUSIONS

The variation of the effective radius implies that elliptical galaxies spend the initial part of their life outside the ‘local’ fundamental plane and only subsequently settle on it.

For massive galaxies ($M_* \geq 2 \times 10^{10} M_\odot$), for which the expansion is mostly due to quasar-driven super-winds, Fig. 1 displays three steps in the evolution: *i*) the end of the quasar phase at cosmic time $t_{\text{QSO}} \simeq t_{\text{vir}} + \Delta t_{\text{burst}}$, which corresponds to the end of the rapid mass loss; *ii*) the intermediate time t_{int} when the stellar component reaches a new virial equilibrium with a larger size; *iii*) the present time t_0 , at which a further, minor increase of the size is achieved due to stellar winds. The initial effective radius has been computed from eq. (3) with $f_\sigma \approx 1.3$.

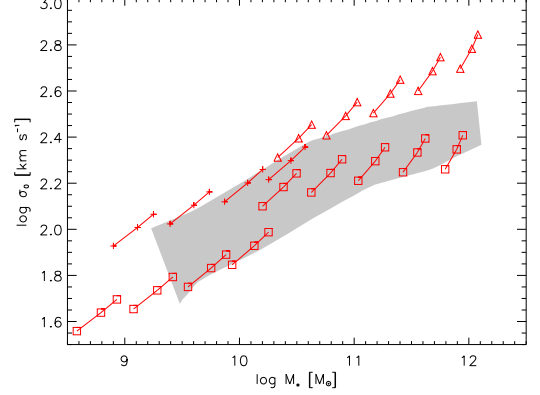


FIG. 2.— Evolution of the central line-of-sight velocity dispersion versus stellar mass. Symbols as in Fig. 1; the same values of z_{vir} and f_σ as in Fig. 1 are adopted. The grey area reproduces the distribution of local data (Gallazzi et al. 2006).

Equation (1) shows that the size expansion can be extremely large as the fraction of expelled gas approaches 50% of the initial mass. However, at variance with the case of star clusters, confined by their own gravitation field, the presence of the DM halo, dynamically dominant at large radii, prevents the disruption and restricts the range of possible final structures of large elliptical galaxies.

The time lapse required to reach the new virial equilibrium can be inferred from numerical simulations of stellar clusters, which show that the system reaches the new equilibrium after about 40 dynamical times (computed for the initial configuration), independently of the initial mass (Geyer & Burkert 2001; Goodwin & Bastian 2006). By scaling up this result, massive galaxies are expected to reach a new equilibrium after ~ 2 Gyr, at $t_{\text{int}} \sim t_{\text{QSO}} + 2$ Gyr (asterisks in Fig. 1). Since then only minor adiabatic mass losses occur, producing slight changes of radius and velocity dispersion (from asterisks to squares). We recall that the quasar activity statistically reaches its maximum at redshift $z \sim 2$, corresponding to a cosmic time $t_{\text{cosm}} \sim 3$ Gyr. The rapid mass loss is then expected to statistically peak at the same redshift, triggering size variations that stabilize after ~ 2 Gyr. Thus the massive galaxies should on the average reach the local size-mass relation at $t_{\text{cosm}} \sim 5$ Gyr, corresponding to $z \sim 0.8$. This result is in keeping with sizes observed at $z \lesssim 1$ (Cimatti et al. 2008) and with results of studies of the Fundamental Plane at $z \leq 0.8$ (Renzini 2006). In the redshift interval $0.8 \leq z \leq 3$ a large scatter in the size–stellar mass relation is expected and indeed observed.

This scenario may appear to be contradicted by observations of Ferguson et al. (2004), who found an average size $r_e \simeq 1.7$ kpc for luminous Lyman Break Galaxies (LBGs) at $z \simeq 4$, while we would expect $r_e \sim 0.5$ kpc, inserting the appropriate masses in eq. (3). However as pointed out by Joung, Chen & Bryan (2008), the apparent effective radius could be a factor of about 3 larger than the intrinsic one, because of the presence of dust in the central star forming regions.

In the case of rapid mass loss, the velocity dispersion of the stars at virial equilibrium scales as $\sigma_* \propto r_e^{-1/2}$. As shown by Fig. 2, the size evolution illustrated by Fig. 1 brings the quite high velocities inferred from the observed values of M_* and r_e in the compact phase, to within the locally observed range.

The structural evolution of low mass E galaxies follows a different path, driven by the slow mass loss due to galactic winds and supernova explosions, because their nuclear activity is of low power. Adopting a Chabrier (2005) Initial Mass

Function (IMF), we find a mass loss of a factor of ~ 2 on a time scale of several Gyrs (the factor is only ~ 1.4 for a Salpeter (1955) IMF); after eq. (2) the size increases by the same factor. However most of the expansion occurs when these galaxies are young. For a Chabrier IMF, already half a Gyr after the baryon collapse the size has increased by a factor of ~ 1.6 (triangles in Fig. 1) and the subsequent expansion is limited to a factor of ~ 1.3 (squares). Thus such galaxies observed at ages $\gtrsim 0.5$ Gyr should exhibit a size quite close to that of local spheroidal galaxies with the same stellar mass. As a consequence, high- z galaxies with $M_* < 2 \times 10^{10} M_\odot$ should also exhibit a smaller scatter in the effective radius–stellar mass relation. They are predicted to have significantly more compact sizes only at ages $\lesssim 0.5$ Gyr, when their star formation rates are of tens M_\odot/yr (see Fig. 1 of Lapi et al. 2006), typical of relatively low luminosity, high- z LBGs. In the adiabatic expansion case the velocity dispersion scales as $\sigma_* \propto r^{-1}$. Again, this brings the high initial velocities within the locally observed range.

As apparent from Fig. 1, we predict significant evolution for galaxies with $M_* \geq 2 \times 10^{10} M_\odot$, well below the threshold of $M_* \geq 5 \times 10^{11} M_\odot$ implied by the semi-analytic model of Khochfar & Silk (2006).

In conclusion we suggest that the rapid mass loss driven by the quasar feedback is the main agent of the size and velocity dispersion evolution of massive spheroidal galaxies. Lower-mass galaxies experience a weaker, but non negligible evolution (of amplitude depending on the adopted IMF), due to mass loss mainly powered by supernova explosions; most of it occurs during their active star-formation phase. Although our calculations have been carried out in the framework of the Granato et al. (2004) model, this evolutionary behaviour is a

generic property of all models featuring large mass loss due to quasar and/or supernova feedback. Observational evidences, some of which are briefly summarized in § 3, suggest that quasar driven high velocity outflows may have removed from the central regions of massive galaxies a gas mass comparable to the mass in stars on a timescale shorter than the dynamical time. If so, simple, model independent, physical arguments, presented in § 2, imply a swelling of the stellar distribution and a decrease of the stellar velocity dispersion. The model contributes detailed, testable, predictions on the evolution of the effective radius and of the velocity dispersion as a function of the galactic age and of the halo mass. It specifically predicts different evolutionary histories for galaxies with present day stellar masses above and below $M_* = 2 \times 10^{10} M_\odot$.

The energy injected by dry mergers into the stellar systems can also enlarge their size. However mergers increase the mass in stars too, and, to first order, move galaxies roughly parallel to the size-mass relation (van Dokkum et al. 2008; Damjanov et al. 2008), while the data show size evolution at fixed mass in stars.

The simple analysis presented in this *Letter* is intended to be a first exploration, sketching a promising scenario for interpreting challenging observational results. This scenario can be tested, on one side, by numerical simulations with appropriate time resolution, properly taking into account the interactions between baryons and DM, and, on the other side, by observations of size and velocity dispersion especially of lower mass high- z galaxies, that are expected to show an evolutionary behaviour different from that of massive galaxies because of the different mass loss history.

This research has been partially supported by ASI contract I/016/07/0 “COFIS”.

REFERENCES

- Biermann, P., & Shapiro, S. L. 1979, *ApJ*, 230, L33
 Chabrier, G. 2005, in *The Initial Mass Function 50 Years Later*, ed. E. Corbelli and F. Palla, *ASSL 327*, Dordrecht: Springer, p. 41
 Cimatti, A., et al. 2008, *A&A*, 482, 21
 Coppin, K. E. K., et al. 2008, *MNRAS*, 389, 45
 Croton, D. J., et al. 2006, *MNRAS*, 365, 11
 Damjanov, I., et al. 2008, *arXiv:0807.1744*
 de Vaucouleurs, G. 1959, *Handbuch der Physik*, 53, 311
 Di Matteo, T., Colberg, J., Springel, V., Hernquist, L., & Sijacki, D. 2008, *ApJ*, 676, 33
 Djorgovski, S., & Davis, M. 1987, *ApJ*, 313, 59
 El-Zant, A., Shlosman, I., & Hoffman, Y. 2001, *ApJ*, 560, 636
 Ferguson, H. C., et al. 2004, *ApJ*, 600, L107
 Ferrarese, L., & Ford, H. 2005, *Space Science Reviews*, 116, 523
 Gallazzi, A., Charlot, S., Brinchmann, J., & White, S. D. M. 2006, *MNRAS*, 370, 1106
 Geyer, M. P., & Burkert, A. 2001, *MNRAS*, 323, 988
 Goodwin, S. P., & Bastian, N. 2006, *MNRAS*, 373, 752
 Granato, G. L., De Zotti, G., Silva, L., Bressan, A., & Danese, L. 2004, *ApJ*, 600, 580
 Granato, G. L., Silva, L., Monaco, P., Panuzzo, P., Salucci, P., De Zotti, G., & Danese, L. 2001, *MNRAS*, 324, 757
 Hills, J. G. 1980, *ApJ*, 235, 986
 Joung, M. K. R., Cen, R., & Bryan, G. 2008, *arXiv:0805.3150*
 Khochfar, S., & Silk, J. 2006, *ApJ*, 648, L21
 Lapi, A., Shankar, F., Mao, J., Granato, G. L., Silva, L., De Zotti, G., & Danese, L. 2006, *ApJ*, 650, 42
 Lutz, D., et al. 2008, *ApJ*, 684, 853
 Magorrian, J., et al. 1998, *AJ*, 115, 2285
 Mao, J., Lapi, A., Granato, G. L., de Zotti, G., & Danese, L. 2007, *ApJ*, 667, 655
 Menci, N., Fontana, A., Giallongo, E., Grazian, A., & Salimbeni, S. 2006, *ApJ*, 647, 753
 Navarro, J. F., Frenk, C. S., & White, S. D. M. 1997, *ApJ*, 490, 493
 Prochaska, J. X. & Hennawi, J. F. 2008 *arXiv 0806.0862*
 Prugniel, P., & Simien, F. 1997, *A&A*, 321, 111
 Renzini, A. 2006, *ARA&A*, 44, 141
 Richstone, D. O., & Potter, M. D. 1982, *ApJ*, 254, 451
 Salpeter, E. E. 1955, *ApJ*, 121, 161
 Sérsic, J. L. 1968, *Atlas de galaxies australes*, Cordoba, Argentina: Observatorio Astronomico, 1968
 Shankar, F., Lapi, A., Salucci, P., De Zotti, G., & Danese, L. 2006, *ApJ*, 643, 14
 Shen, S., Mo, H. J., White, S. D. M., Blanton, M. R., Kauffmann, G., Voges, W., Brinkmann, J., & Csabai, I. 2003, *MNRAS*, 343, 978
 Silk, J., & Rees, M. J. 1998, *A&A*, 331, L1
 Simcoe, R. A., Sargent, W. L. W., Rauch, M. & Becker, G. 2006, *ApJ*, 637, 648
 Tacconi, L., et al. 2008, *ApJ*, 680, 246
 Toft, S., et al. 2007, *ApJ*, 671, 285
 Trujillo, I., et al. 2004, *ApJ*, 604, 521
 Trujillo, I., Conselice, C. J., Bundy, K., Cooper, M. C., Eisenhardt, P., & Ellis, R. S. 2007, *MNRAS*, 382, 109
 van Dokkum, P. G., et al. 2008, *ApJ*, 677, L5